Chapter 6
Testing Concrete Since Setting Time Under Free and Restrained Conditions

Brice Delsaute and Stéphanie Staquet

Abstract Restrained deformations in concrete structures induce the development of stresses and sometimes cracking. Therefore the whole service life of concrete structures is influenced by the appropriate consideration of the early age behaviour of concrete under restrained conditions. For that reason, several devices were developed in the past to characterize the risk of cracking of cement-based materials. In the 1990s, a new experimental concrete testing concept has been designed: the Temperature Stress Testing Machine (TSTM). The device is able to monitor several parameters such as the age of cracking, the stiffness development and the stress relaxation. Between 1990 and 2010, less than fifteen laboratories worldwide have developed or acquired this kind of experimental equipment. All devices bear some similarities but major differences remain in the test set up designs, in the testing processes and also in the scale of the material used. This chapter summarizes all existing technics used to assess the behavior of concrete under restrained deformation, a comparison of the different existing TSTM is presented. New advanced techniques aim at monitor the cracking risk of cement-based materials such as the active ring test or the elliptical ring test are also presented.

Keywords Restrained deformation · Cracking · Shrinkage · Early age · Creep/relaxation

6.1 Introduction

As explained in detail in the Chaps. 4 and 5, concrete has the particularity to be a complex material for which its properties continuously change. It evolves from a

B. Delsaute (✉) · S. Staquet
Service BATir, LGC, Université Libre de Bruxelles (ULB), Brussels, Belgium
e-mail: bdelsaut@ulb.ac.be

nearly liquid state to a viscoplastic material within a few hours, followed by the setting of the concrete. Then the mechanical properties start to develop and the material exhibits viscoelastic behaviour. During the first days after mixing, the evolution of the concrete properties is very intense. This period is called the early age. Finally, the concrete properties continue to evolve on a period counted in years. Concrete has also another important specificity coming from its time-dependent properties. At early age, the development of the free deformation induced by desiccation (drying shrinkage) and hydration (thermal and autogenous deformation) are generally partly or fully restrained which leads to the development of internal stresses. For the determination of the stress under restrained condition, the development of the elastic and creep properties are important parameters. To model the behaviour of the concrete, the total strain of the concrete ε_{tot} are decomposed as the sum of 5 terms: the autogenous strain ε_{au}, the thermal strain ε_{th}, the drying strain ε_{ds}, the elastic strain ε_{el} and the creep strain ε_{cr} (Eq. 6.1). Creep strains are also divided in two terms. The first term is related to the behaviour of concrete under sealed condition and the second term is caused by the drying phenomenon. Both are called basic creep and drying creep respectively. The constitutive law related to the viscoelastic behaviour of cement based materials is given in Eq. 6.2 for a constant uniaxial stress σ where t is the age of the concrete, t′ the age of the concrete at loading, $J(t, t')$ is the compliance function, $E(t')$ is the elastic modulus and $C(t, t')$ is the specific creep.

$$\varepsilon_{tot} = \varepsilon_{au} + \varepsilon_{th} + \varepsilon_{ds} + \varepsilon_{el} + \varepsilon_{cr} \tag{6.1}$$

$$\varepsilon_{el}(t') + \varepsilon_{cr}(t, t') = \sigma \cdot J(t, t') = \sigma \cdot \left(\frac{1}{E(t')} + C(t, t') \right) \tag{6.2}$$

For concrete structures, the evolution of the restrained strains and the associated stress development depend on the type of structure (thin or massive), the exposition of the structure to the environment (e.g. sealed by the formwork or exposed to drying) and the composition of the concrete (e.g. type of cement, W/C …). For illustration, two opposite situations are presented in the Fig. 6.1. On the left, the first case corresponds to a thin concrete element exposed to drying since the casting. This is for example the case of concrete slab for which normal strength concrete is generally used. In such case, low thermal changes are caused by hydration. Thus the development of the free deformation is mainly driven by the autogenous strain and the drying shrinkage (Bendimerad et al. 2020; Delsaute et al. n.d.). This corresponds to a global shrinkage of the concrete element as shown in Fig. 6.1, left. As a result, tensile stress is induced in the concrete element when the free deformation is restrained. The second case refers to a massive structure for which the free deformations are mainly composed of the autogenous and thermal strain. Two periods are observed in the development of the free deformation: a heating period followed by a cooling one (Fig. 6.1, right) as explained in (Delsaute and Staquet 2019; Delsaute et al. 2017). The heating period begins just after the final setting when the mechanical properties of concrete start to develop. During and after the setting, the heat flow of
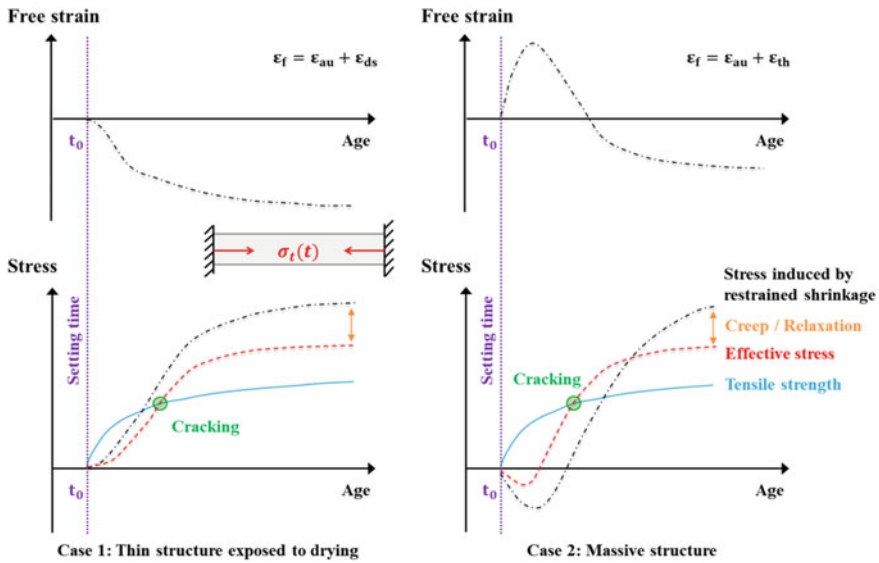
Fig. 6.1 Evolution of the stress induced by the restriction of the concrete free strain for thin structure exposed to drying (left) and massive structure [right (Delsaute et al. 2017)]

the cement is very intense which leads to an increase of the temperature inside the concrete element and as a result to an increase of the thermal strain. In the meantime, autogenous strain starts to develop. No systematic tendency can be given for the autogenous strain, because during the heating period, autogenous deformation results in swelling or shrinkage according to the mixtures proportions and content (Benboudjema et al. 2019; Bentur 2003b; Staquet et al. 2019). However thermal strains are generally higher than autogenous strain (especially for massive structures) and thus a general swelling of the concrete occurs during the heating period. The cooling period starts when the heat flow of the cement decreases strongly or when the formwork is removed (according to the massivity). During this period, both autogenous and thermal strains decrease. As a result of the restriction of the strains of concrete, stresses are induced (Fig. 6.1, right). During the heating period, concrete element is in compression and inversely during the cooling period the concrete is submitted to tension.

The impact of viscous properties at very early age, in case of restrained deformation, is highlighted on the development of the stress as shown in Fig. 6.1 (red curve, viscoelastic stress). In the case of a thin concrete element exposed to drying, creep and relaxation have the positive effect to reduce the development of the tensile stress, especially at very early age when the creep/relaxation phenomena are very important. In the case of massive concrete element, in a general view, no consideration of creep/relaxation leads to a global overestimate of the stress. Thus creep/relaxation seems to play a general positive role for the design of massive concrete structures

at early age. However, at very early age, the creep/relaxation amplitude is very significant and reduces strongly the compressive stresses. Then, during the cooling period, stresses switch rapidly in tension. During this period, an underestimation of the creep/relaxation phenomenon leads to an underestimation of the tensile stresses which can cause cracking in the concrete structure. Hence it is important to consider correctly the creep and relaxation phenomena since final setting time for the study of the behavior of cement based materials under restrained conditions. All the concrete properties depend on the composition of the concrete. For high strength concrete, the development of the autogenous and thermal strain is higher and thus those compositions are more sensitive to a cracking risk.

The cracking sensitivity of cement based materials is therefore defined by the type of structure, the environmental conditions and the concrete compositions. Moreover the early age and long term concrete properties are dependent of the massivity of the structure and the environmental exposition. This makes the study of the cracking sensitivity of concrete structure a challenging task when considering the evolution of the whole concrete properties for the determination of the stress inside a concrete element when its deformation is restrained. For that reason, several tests have been developed to estimate the cracking risk of cementitious materials, such as the ring tests, the plate tests and the passive longitudinal tests (Bentur 2003a). Generally, these experimental tests allow determining the number of cracks, their width and the stresses evolution inside the concrete sample. However, this evolution strongly depends on the geometry and the stiffness of the material used to obtain the restrained conditions. Thus, these devices can be used for qualitative means which are useful for comparison of the cracking sensitivity of different concrete compositions but are not sufficient alone for the study of the mechanisms involved in the cracking risk. To eliminate these drawbacks, an active longitudinal test named Temperature Stress Testing Machine (TSTM) was developed from the beginning of the 1980s. With this device, a full or a partial degree of restriction of the concrete sample can be obtained by means of the application of a compressive/tensile stress on a dog-bone shaped concrete specimen to keep its length constant with a manual or an automatic system.

The present chapter summarizes the analysis of the development of the TSTM's at the Université Libre de Bruxelles. Based on this analysis, a revisited TSTM and experimental procedure have been developed to study the sensitivity to cracking of concretes. The present chapter is structured in five main sections (apart from the present introduction). The second section of this chapter is related to the presentation of the tests rig developed for the determination of the stress of concrete under restrained condition. The third section explains the principle of a TSTM, the history of the TSTM development in a dozen of other laboratories as well as a synthesis of the key elements in the design of a TSTM. In the fourth section, the development and the new technical advances performed on the TSTM during this last decade at ULB are presented. Several new applications of the TSTM are introduced in the fifth section. Finally, conclusions are given in the sixth and ultimate section of the present chapter.

6.2 Test Rig Designed for the Study of the Risk of Cracking of Cement Based Materials

Restrained shrinkage tests can be divided mainly into two categories: passive and active restrained shrinkage tests. In case of passive restrained shrinkage test, there is no control of the degree of restraint of the concrete strain in the test setup. The degree of restraint is driven by the difference of stiffness of the restraining frame and the concrete one. For that reason, active devices, for which the restraining part of the device is controlled (in terms of displacement, force or temperature controlled), have been developed.

6.2.1 Passive Restrained Shrinkage Test

As presented by Bentur and Kovler in (Bentur 2003a), mainly four passive restrained shrinkage tests have been developed, namely the plates test, the substrate restrained test, the longitudinal test and the ring test.

6.2.1.1 Plate Test

The plate test is mainly used in the study of plastic shrinkage and it quantifies the performance of concrete by estimating the extent of its cracking by means of the average and maximum width of the crack, of their total length, their total area and number per unit area (Bentur 2003a). For this test, the concrete is poured into a slab mold (Fig. 6.2). In addition to the relative friction in the contact zone between the mold and the slab, the restrained is mainly induced by the presence of steel reinforcement embedded in the slab and fixed to the edges of the plate.

Fig. 6.2 Scheme of the plate test (Yokoyama et al. 1994)
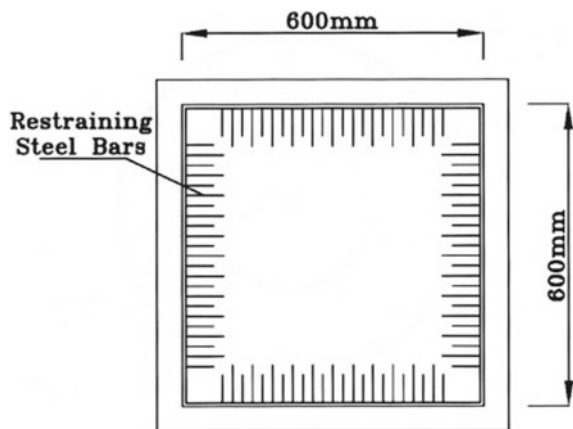
Fig. 6.3 Substrate restrained tests developed for the study of the curling (Bentur 2003a)
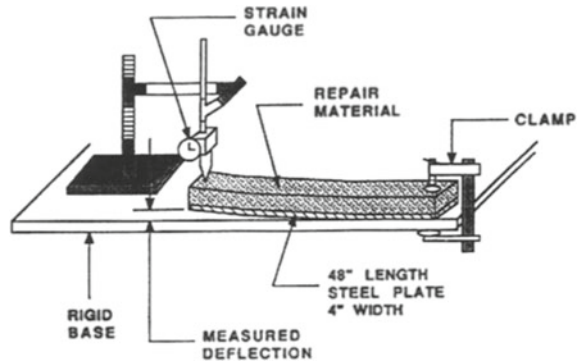
6.2.1.2 Substrate Restrained Test

Substrate restrained tests were developed to simulate the restraint of the deformation of fresh mortar or concrete used for the reparation or the resurfacing of concrete structure. Two types of test were developed in order to study the risk of cracking or curling. To study the risk of cracking, a fresh layer of mortar or concrete is casted on a hardened concrete layer (Banthia et al. 1993, 1995, 1996) or a steel layer (Vaysburd et al. 2001) and is exposed to ambient air (Vaysburd et al. 2001) or to a controlled temperature and relative humidity (Banthia et al. 1993, 1995, 1996). This quantifies the performance of mortar/concrete by estimating the extent of its cracking by means of the number of cracks, the average and maximum width of the crack, time of cracking and detachment from the substrate layer. To evaluate the risk of curling, a rectangular layer of the material is casted alone or on a steel substrate and the top part of the specimen is exposed to ambient environment. One end of the specimen is embedded while the other one is free. The vertical displacement of the free extremity or at mid-span is measured to evaluate the performance of the material as illustrated in Fig. 6.3 (Vaysburd et al. 2001). At the structural scale, similar test setups were designed for the study of the curling phenomenon induced by the differential shrinkage between the bottom and the top surface of slab [see e.g. (Jaafri et al. 2019)].

6.2.1.3 Longitudinal Test

Two passive longitudinal tests have been designed:

– Longitudinal-qualitative: In this test, the longitudinal geometry of the apparatus is used as a restriction to the free deformations of the concrete element and it only allows quantifying the cracking by measuring the width of the cracks and the total length of cracking.
– Longitudinal-quantitative passive: In addition to cracking measurement, this device is able to determine the restriction forces and stresses developed within
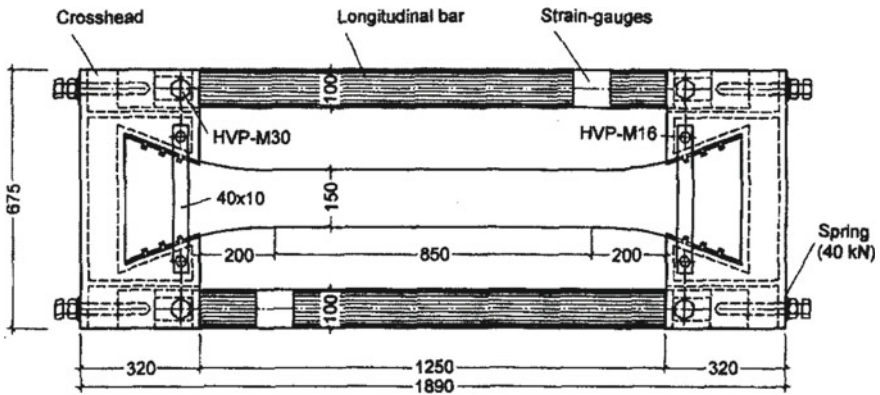
Fig. 6.4 Longitudinal passive restrained shrinkage test (RILEM TC 119-TCE 1997)

the material. This test is considered as passive because the restriction is obtained by means of external bars of constant length (Fig. 6.4). In this device, concrete deformations are not completely restrained and thus the length of the specimen is still slightly variable. Deformation gauges are placed on the metal columns and quantify the existing displacement. The restraining stresses are therefore calculated from the strain gauge data with consideration of the steel properties of the outer columns of the device and the dimensions of the section of the concrete specimen. In addition, for the study of mass concrete element, insulation can be placed around the sample and the mold can be regulated in temperature (Bentur 2003a).

Longitudinal-quantitative passive tests were also developed at the structural scale. In the frame of the French national project CEOS (CEOS.fr n.d.; Delsaute et al. 2013), 3 blocks subject to restrained shrinkage were tested. The dimension of each body is 6.1 m × 1.6 m × 0.8 m (Fig. 6.5). These tests were performed in order to improve the design of massive concrete structure, specifically the crack pattern of special

Fig. 6.5 Restrained shrinkage test at structural scale (CEOS.fr n.d.)

concrete structures. For that reason, reinforcement ratio (0.6 and 2%) and concrete cover (50 and 70 mm) vary from one block to another.

6.2.1.4 Passive Ring Test

The ring test is the most common device used for the study of the restrained shrinkage. Plastic shrinkage cracking and shrinkage cracking can be assessed with the ring test. The device is composed of a ring (generally in steel) around which a concrete ring is casted. During the test, the free shrinkage of the concrete ring is restrained by the inner ring. It quantifies the performance of the material by estimating the age of cracking, number of crack and the average and maximum width of the cracks. When lateral faces of the concrete ring are exposed to drying, the test simulate the behavior of an infinitely long structure subjected to restriction (Weiss and Shah 2002). As highlighted by Kanavaris et al. (2019), the main parameters varying in the design of a ring test are related to the test apparatus, the environment and the test protocol. For example, the dimensions of both rings depend on the standards and the type of material studied (i.e. cement paste, mortar or concrete). All variable parameters are synthesized in the Table 6.1.

For illustration, the dimensions of the ring test according to the AASHTO standard (Darquennes et al. 2006) are shown in Fig. 6.6.

Based on the geometry of the test and the measurement of the deformation in the internal part of the inner ring, analytical solutions were developed for the calculation of the elastic hoop stress of concrete [see e.g. (Hossain and Weiss 2004, 2006; Kovler and Bentur 2009; Weiss et al. 2000)]. A comparison of the different analytical approach fund in the literature is performed in (Kanavaris et al. 2019). Recently, a critical review of the development of the ring test was carried out by Kanavaris et al.

Table 6.1 Main parameters in the design of a ring test

Test apparatus	Environment	Test protocol
• Dimension of the restraining core (inner and outer radius, hollow/solid and height) • Dimension of the restrained ring (inner and outer radius and height) • Nature of the restraining ring (e.g. stainless steel, Invar) • Nature of the restrained ring (cement paste, mortar or concrete) • Degree of restraint	• Curing temperature (ambient or controlled) • Relative humidity (ambient or controlled)	• Formwork removal age • Drying direction (circumferential, top and bottom, top, all 3 sides exposed or all 3 sides sealed)
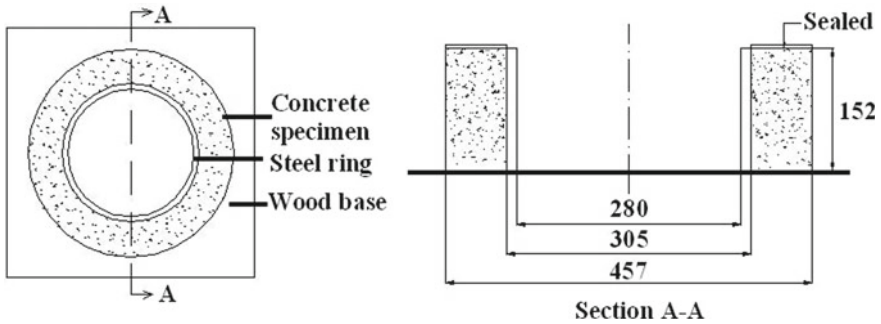
Fig. 6.6 Ring test according to AASHTO standard (Darquennes et al. 2006)

(2019). From this review, new recommendations in the testing method are addressed according to the type of application.

Other alternatives to the conventional ring test were developed to accelerate the development of cracking. This improvement is interesting since cracking can occur after several months for Portland cement-based concretes [see e.g. (Darquennes et al. 2006)]. For example, Dahl (Bentur 2003a) encloses the concrete ring between two steel rings. The outer ring is provided with ribs causing an increase in the stresses within the material. Other authors (Turcry 2004) have notched their concrete ring, which allows obtaining relatively short material cracking times. Recently, several authors have also proposed to replace the steel ring by an elliptical ring for which stress development is higher in the minor radius of the ellipse (Dong et al. 2018; He et al. 2004; Zhou et al. 2014). For the consideration of the restrained of the swelling deformation, Weiss et al. (2008) have added an outer restraining steel ring. This device is called dual ring test.

6.2.2 Active Restrained Shrinkage Test

In order to control the degree of restraint of the concrete strain during the test, active restrained shrinkage tests have been developed. Three methods were adopted: the control in displacement, in force and/or in temperature of the concrete specimen. Mainly, two types of device were developed: active ring tests and active longitudinal tests.

6.2.2.1 Active Ring Test

The active feature of the ring test is related to controlled temperature changes imposed during the test. As the coefficients of thermal expansion (CTE) of the restraining ring(s) and the concrete ring are different, a change in temperature restrains the

deformation or imposes an expansion of the concrete ring. First, Kovler et al. (1993) have replaced the hollow steel ring by an active-expansive core with a CTE higher than concrete. When increasing the temperature, additional tensile stresses were therefore induced in the concrete ring which shortened the age of cracking. Then Schlitter et al. (2010a, b) have developed a dual ring test for which both restraining ring are made of Invar. The whole device is placed in a highly insulated chamber which is controlled in temperature. As the CTE of Invar is very low, the restraining boundaries of the concrete ring are nearly constant. For the study of massive concrete element, Briffaut et al. (2011a, b) used a thermally-active ring. The restraining ring is made of brass (the CTE is about 3 times higher than concrete) and is regulated in temperature thanks to water circulation into it. Contrary to Schlitter's system, the restraining boundaries are moving during the test. Recently, Bourchy (2018) has developed a dual ring test for which both restraining rings are made of Invar and are thermally-controlled (the temperature evolution correspond to the temperature recorded during a quasi-adiabatic calorimetry test).

6.2.2.2   Active Longitudinal Test

The active part of the longitudinal test is related to the control in force or in displacement of one of the extremity of the concrete specimen. Two configurations of the specimen were developed: vertical and horizontal test rig. These devices, named TSTM (Temperature Stress Testing Machine), are described in detail in the next paragraph.

6.3   The TSTM (Temperature Stress Testing Machine)

6.3.1   Principle of TSTM's

The determination of the different concrete parameters is based on the hypothesis of independence of the deformation components. The total deformation is assumed to be equal to the sum of the elastic ε_e, creep ε_{cr}, thermal ε_{th} and shrinkage ε_{sh} deformations, as expressed in Eq. 6.1. The degree of restriction of deformations is equal to zero if this sum is null. For the study of the evolution of the different parameters, compensation cycles are used with a threshold value of deformation ε_l equal to a few microns (or microstrains) for applying the restriction conditions during the experimental test (Fig. 6.7). As soon as this value is exceeded, a load is applied on the concrete sample to cancel the deformation. Then, the concrete sample can shrink again and the load is kept constant but the stress/strength ratio increase with the time. Then another compensation cycle begins (Fig. 6.8). So the cycles succeed to themselves during the entire test until cracking of the sample occurs.
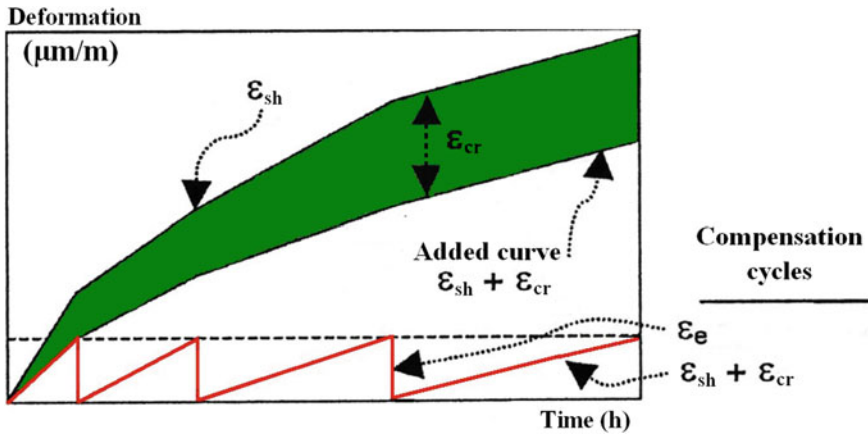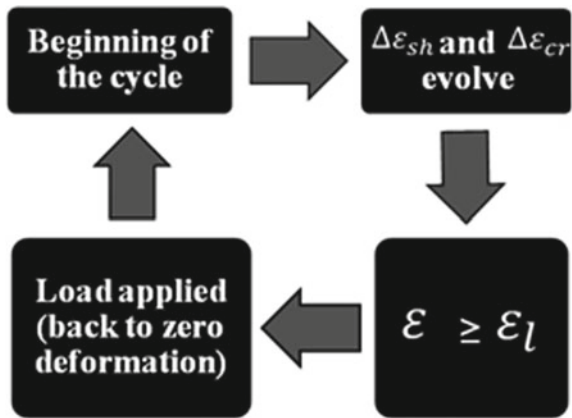
Fig. 6.7 Schematic description of the compensating cycles to obtain the restriction conditions with the TSTM (Kovler 1994)

**Fig. 6.8** Steps inside each compensating cycle

Following these compensation cycles, the sum of all elastic deformations is equal to the sum of the restrained deformations, i.e. creep and free strain (Fig. 6.7). From these experimental results, the creep deformation can be calculated as the difference between the curves of free strain and restrained deformations. Another parameter can also be estimated from this test: the relaxation stresses.

6.3.2 History of the Development of TSTM's

One of the oldest TSTM equipment was developed in the beginning of the 1980s by Springenschmid et al. (1994) at the Technical University of Munich in Germany. In

this equipment, the dog-bone sample is characterized by a square cross section 150 × 150 mm^2 and a length equal to 1500 mm (Schöppel et al. 1994). The restriction conditions were obtained for a deformation threshold equal to 1 μm and were applied when the material is characterized by a significant stiffness. This time is the moment when the stresses begin to develop inside the concrete sample. For the experimental tests performed with this TSTM, the displacement was measured by means of steel bars placed in the concrete sample in its central part at an interval equal to 500 mm. The same device was used for measuring the free shrinkage. This boundary condition was obtained by cancelling the force applied on the concrete sample when the stress inside the concrete reaches a value equal to 0.01 MPa. It appears that this first device is already characterized by two main parameters limiting the artifacts of restrained shrinkage measurements: a thermal regulation of the concrete sample and a system of deformation measurement directly placed on the concrete sample. At the same period, Paillière et al. (1989) also developed a TSTM equipment in which a dog-bone sample was tested in vertical position. However, this device cannot be used at early age because its specimen must be firstly casted in a horizontal mold before its placement in the TSTM. Moreover, this device is not equipped with a thermal regulation and the vertical position of the sample can lead to an early cracking localized in its upper part as a consequence of the non-uniform stress distribution arising from the hanging self-weight. These first TSTM devices allow underlining several major parameters which must be taken into account for their design: the position of the deformation measurement system, the presence of a thermal regulation on the concrete sample and the sample position (Fig. 6.9).

At the beginning of the 1990s, a TSTM was set up at the Israel Institute of Technology (Technion) at Haifa (Bloom and Bentur 1995; Igarashi et al. 2000). The free and restrained shrinkages were simultaneously measured on samples that differ only by one of their extremities, which is free for the sample used for measuring the free shrinkage and which is piloted in the other case. With this equipment, the
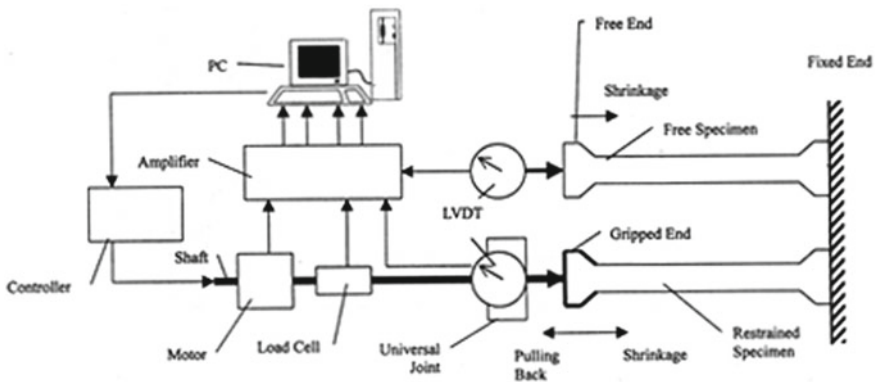
Fig. 6.9 System for monitoring free and restrained shrinkage at the Israel Institute of Technology (Igarashi et al. 2000)

deformation was measured by means of LVDT sensors placed on the moving head of the restrained sample. It has been demonstrated that this kind of method can generate some artifacts of displacement measurements (Altoubat and Lange 2002). Indeed, the interaction between the grip and the concrete sample can pollute the displacement measurements and induces a decrease in the restrained degree of sample. Moreover, a sliding between the sample and the grip is always possible. During these tests, the thermal regulation was provided by means of the room air conditioning only.

Several tests on TSTM's devices were carried out for several applications at the Norwegian University of Sciences and Technology (NTNU) at Trondheim in Norway (Bjontegaard 1999; Ji et al. 2018) and at the Technical University of Delft (DTU) in the Netherlands (Lokhorst 1998; Lura 2003). Tests on high performance concrete were realized at NTNU. Bjøntegaard investigated the effect of different isothermal curing temperatures and realistic histories of temperature on high performance concretes (Bjontegaard 1999). For this purpose, they equipped the TSTM mold with a thermal regulation system. This system consists of copper pipes disposed along the mold. It allows obtaining an isothermal temperature of 20 °C after about 1–2 h. Moreover, the temperature increase due to the hydration of a Portland cement concrete sample is limited to 1.5 °C. However, a thermal gradient in the longitudinal and transverse axis always exists because the temperature of the liquid coolant varies from its initial temperature during its travel following its calorific losses. They also demonstrated that the value of the deformation threshold directly affects the value of Young's modulus calculated from each compensative cycle. From these first experimental results, it seems better to evaluate the value of the elastic modulus from complementary tests.

More recently, several university laboratories, namely at the University of Illinois at Urbana Champaign in the USA (Altoubat and Lange 2001), the Swiss Federal Institute of Technology in Lausanne in Switzerland (Kamen et al. 2008), the Monash University in Australia (Aly and Sanjayan 2008), the University of Tokyo in Japan (Kishi and Lin 2008) and the Polytechnical School of Sao Paulo in Brazil (Melo Neto et al. 2007), equipped themselves with a TSTM equipment. Although these equipments bear some similarities (a dog-bone sample, a horizontal position for the specimen …), it appears that their design and their test method differ by several points. These differences are indicated in the Table 6.2 and summarized below:

– Position (top or sides of the straight part of dog-bone specimen) and accuracy of the LVDT sensors, as well as the gauge length generally included between 500 and 750 mm.
– Size of the sample: length of the straight part (about 1000 mm), cross section (from 40×40 mm^2 to 150×150 mm^2).
– Existence of a thermal regulation system around the specimen for stabilizing the temperature at the beginning of the test, keeping an isothermal temperature during the test and limiting the thermal gradient in the sample.
– System for controlling the displacement of concrete sample during the compensation cycles (manual or automatic).
– Kind of device for monitoring the free shrinkage (rectangular or dog-bone sample).

Table 6.2 Differences between TSTM systems

References	Springenschmid et al. (1994)	Igarashi et al. (2000), Bloom and Bentur (1995)	Bjontegaard (1999)	Grazia (1999), Charron (2003)	Lokhorst (1998), Lura (2003)
Test start	0.01 MPa	24 h	Setting time	24 h	8 h
Deformation threshold (μm/m)	2	5	0.86	6	6
Sample cross section	150 × 150 mm	40 × 40 mm	90 × 100 mm	50 × 50 mm	150 × 150 mm
Sample length (mm)	1500	1000	1000	1000	1000
Gauge length (mm)	500	–	700	750	750
Deformation measurement	Side	Mobile head	Side	Top	Side
Thermal regulation	Yes	Room conditioning	Yes	Yes	Yes

– Value of the deformation threshold used for obtaining the restriction conditions which varies from a value close to 0 (0.1; 0.6 μm/m) to a value equal to a few microstrains (4; 6 μm/m).
– Starting time of the restrained shrinkage test: setting of material, stress threshold, material age …

These TSTM devices allowing the study of the visco-elastic behaviour of concrete at early age respect the recommendations of the technical committee Rilem 42-CEA (Rilem 42-CEA 1981) for uniaxial tensile testing of concrete at early age:

1. The experimental tests are performed horizontally to avoid the dead load effect of specimen.
2. The friction between the sample and the mold is minimized by using specific material like the combination of Teflon and plastic film.
3. The sample is prismatic and its extremities are larger than its central part.
4. The length of the longitudinal central part of the sample is at least four times higher than that of its cross section.

So, these different parameters have been taken into account in the design with the integration of a thermal regulation inside the mold of the TSTM sample at the laboratory of the Université Libre de Bruxelles (ULB). Moreover, an appropriate test method for studying the restrained shrinkage has been also chosen to limit the early cracking of the sample. The details of the revisited TSTM system are presented in the next paragraph.

6.4 Design Testing System

6.4.1 Test Setup

A revisited TSTM system was developed (since 2006) in the laboratory of civil engineering at the ULB for testing concrete since setting time under free and restrained conditions. For this purpose, the testing machine is a Walter + Bay LFMZ 400 kN electromechanical testing setup. The machine is totally programmable and controlled (force and displacement of each sensor) by computer. The machine is composed by a fixed steel head, a central unidimensional part and a moving end. The moving end is controlled by a motor moving the steel head.

The transition area between the ends and the central part is characterized by a rounded shape in order to minimize a possible stress concentration and the risk of premature cracking in this zone. In the central part where the measurements of the displacements are taken, the stress field has been computed with finite element analysis and it was shown that the stress filed is homogenous (Baesens and Delsaute 2010). The shape of the mold is a dog-bone (Table 6.3). The dimensions of the cross section are 100×100 mm^2 in the central part and 300×100 mm^2 at the ends. The total length of the straight part equals to 1000 mm. With these dimensions, it is possible to perform tests for concrete with a maximal aggregate size of 20 mm. The shape of the mold induces stress concentration in the junction between the head and the straight part of the specimen. The failure of the sample takes often place in this part of the sample. For the study of the creep at high stress level, the stress concentration at the junction between the head and the straight part of the sample has to be decreased. For these reasons, the geometry of the head was replaced (Fig. 6.10).

The fresh concrete is cast inside the mold until a level of 100 mm. One T type thermocouple is placed in the middle of the sample during the casting, at each end and at mi-length of the central part of the mold. The temperature of the sample is controlled by a flow of a specific liquid for thermal regulation circulating on all the sides of the specimen. A plastic sheet is placed, before casting, in the mold to ensure sealed conditions. Moreover, the plastic sheet helps also to reduce, with the presence of Teflon, the friction between the sample and the mold. The walls of the mold are made of aluminum (Fig. 6.11) which was chosen for its high thermal conductivity (237 W/m K) and its low density (2700 kg/m^3). The deflection of the mold is very limited (± 2 mm) and the isothermal conditions are ensured thanks to a fast heat

Table 6.3 Dimensions of the specimen in the TSTM device

|		
Length of the span (m)	1	
Width of the span (m)	0.1	
Radius of curvature (m)	0.5	
Width of head (m)	0.3	
Length of head (m)	0.1	
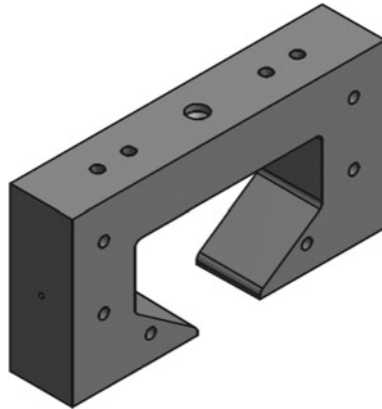
Fig. 6.10 New geometry of the head
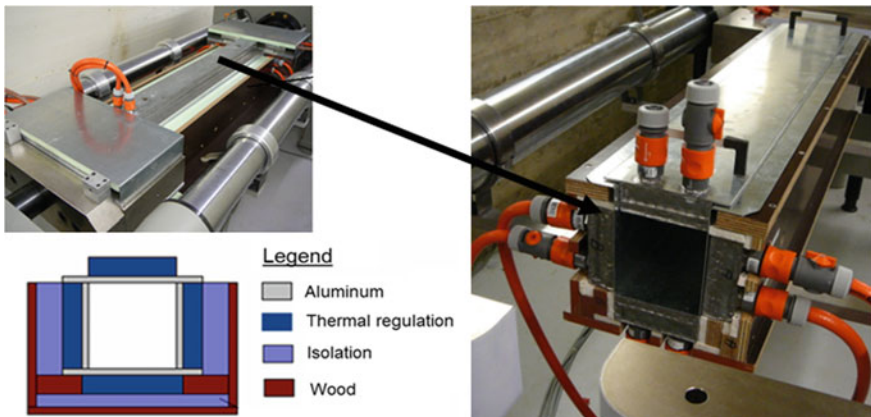
Fig. 6.11 Thermal insulation

transfer with the zinc boxes. A specific liquid for thermal regulation flows inside zinc boxes beams which are placed all around the central part and on the ends and under them. Each box is independent and has its own water input and output system. A thermal insulation limits exchanges with the ambient environment. The equipment is located in an air-conditioned room with a control system of the temperature and the relative humidity.

In addition to the creep and elastic deformations, thermal and shrinkage deformation must also be known. For this purpose, a dummy mold was built for the measurement of the thermal and free shrinkage deformations. This mold has exactly the same geometry as the first one. The only difference is the total free movement of one of the ends (Fig. 6.12).
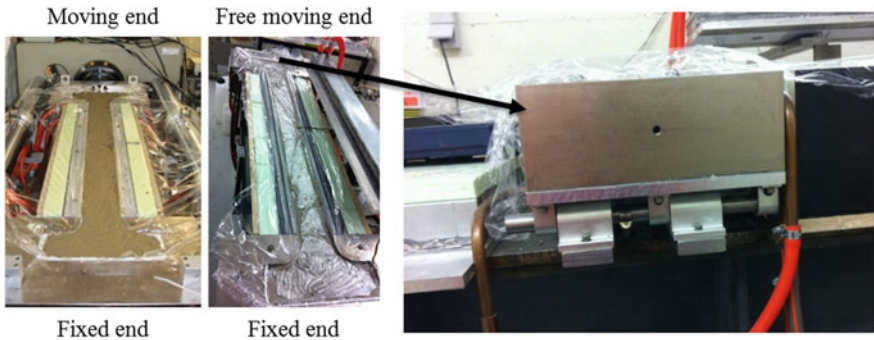
Fig. 6.12 Left to right: mold (boundary conditions)—dummy mold (free moving end thanks to ball bearings)

In this equipment, several instrumentations were developed at ULB for the monitoring of the concrete deformation. For the first instrumentation, the displacement is measured by means of two transducers (Solartron LE12). The displacement sensors are placed on invar supports which are fixed on a rigid frame made of aluminum tubes externally supported by the TSTM (Fig. 6.13). The distance between both sensors is 750 mm (where the stress field is homogenous in the sample). These sensors are characterized by a measuring range of 12 mm and accuracy of about 0.4 μm.

Invar rods are anchored in the concrete at a depth of 50 mm. The link between the concrete displacement and the sensor is then assured. These invar rods are characterized by a low dilatation coefficient limiting the effect of ambient temperature on the deformations measurement. They are kept in their initial position thanks to a brass ring before the beginning of the test. The horizontality of the TSTM device is an advantage for the efficiency of the casting. Moreover, sensors are well anchored at mid-height and not in the superficial layer of the sample, what could have induced an error by a possible different behavior between the core layer and the superficial layer (less aggregates presence) (Fig. 6.14).
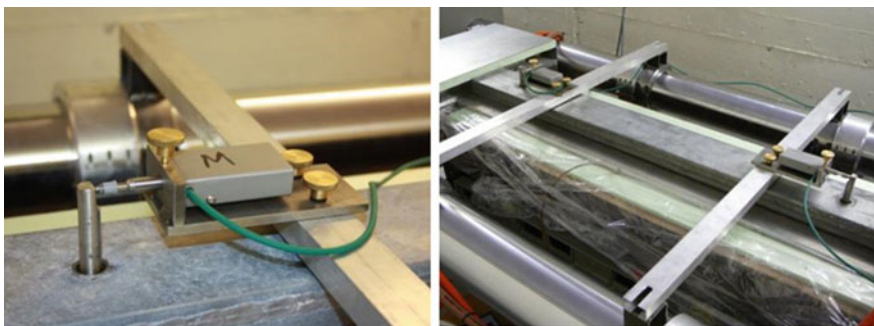
**Fig. 6.13** Displacement sensors in the central part of the specimen

(a)
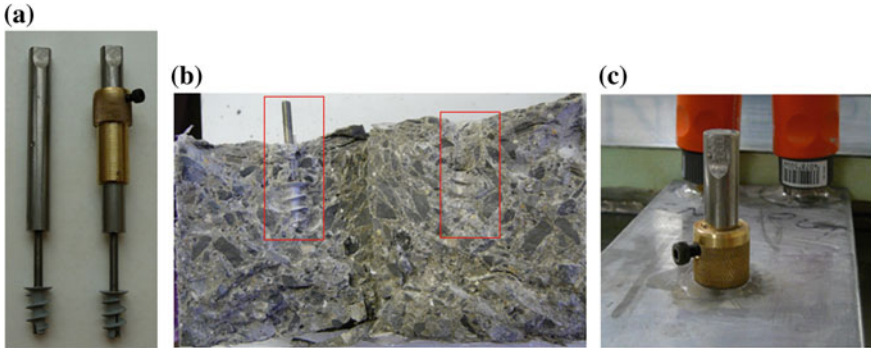
Fig. 6.14 Stem (Invar, threaded stem in steel) with plastic plug and brass ring (**a**)—incorporate stem in the concrete (**b**)—embedding system in steel of the Invar rod (**c**) (Darquennes 2009)

In order to improve the displacement measurement since setting time and to perform relaxation test, different changes were carried out on the instrumentation. The aluminum tubes connecting the columns of the test device and the displacement sensors have been replaced by solid steel bars for which the thermal inertia is higher and the CTE is lower. The influence of thermal variation in the room is therefore lower on the measurement of displacements. Displacement sensors in the central part of the specimen were replaced by Foucault current's sensors (without contact sensor) (Fig. 6.15). Sensors have a resolution of 0.014 μm and a measurement range of 2 mm.

These sensors have two advantages. Firstly, the absence of contact between the sensors and the mold avoids measurement artifacts induced by the spring of the LVDT sensor when the stiffness of the concrete is very low. Secondly, an instantaneous Volt conversion in micrometer of the sensors allows piloting the TSTM system with the displacement directly measured in concrete. A real time subtraction between the

Fig. 6.15 Displacement sensor without contact

$$\frac{S1 + S2}{750\ mm} = \varepsilon_e + \varepsilon_c + \varepsilon_{th} + \varepsilon_s \qquad \frac{S3 + S4}{750\ mm} = \varepsilon_{th} + \varepsilon_s$$
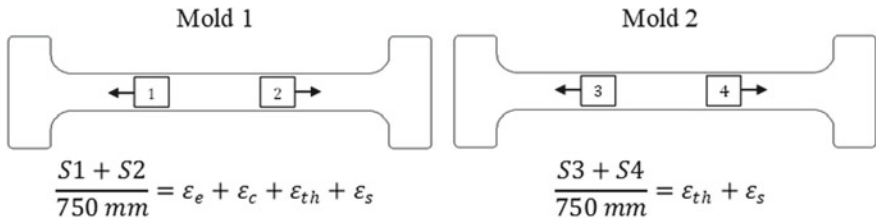
Fig. 6.16 For relaxation test, TSTM device is controlled by (S1 + S2)–(S3 + S4) which corresponds to creep and elastic deformations

deformation of the specimen in the TSTM and the specimen in the companion (passive) mold allows piloting the TSTM system on basis of the mechanical parameters excluding the free deformations due to thermal variations ε_{th} and due to shrinkage ε_{sh}. So, the direct measurement of the elastic ε_e and creep ε_c deformations or the relaxation stresses is possible with the simultaneous use of the first and the second mold as illustrated in Fig. 6.16.

Without contact sensors are very sensitive to the air conditioning. A good protection of the sensor is needed. Figure 6.17 shows the perturbation caused by the air conditioning on the sensor when repeated loadings in tension are applied on a concrete sample (Delsaute 2016). The different "waves" are in direct relation with the air conditioning. The use of displacement sensor with contact as LVDT decreases the impact of the air conditioning. However this problem was solved by protecting the sensor from the air conditioning. A wood box was designed in order to protect completely the sensor from the ambient air.

For some tests, the failure occurs in the straight part of the specimen where the anchorage is placed. To decrease the risk of failure and to avoid a preliminary damage in this zone, the plastic plug was removed to limit the reduction of the concrete cross section. However different problems were observed for the measurement of the
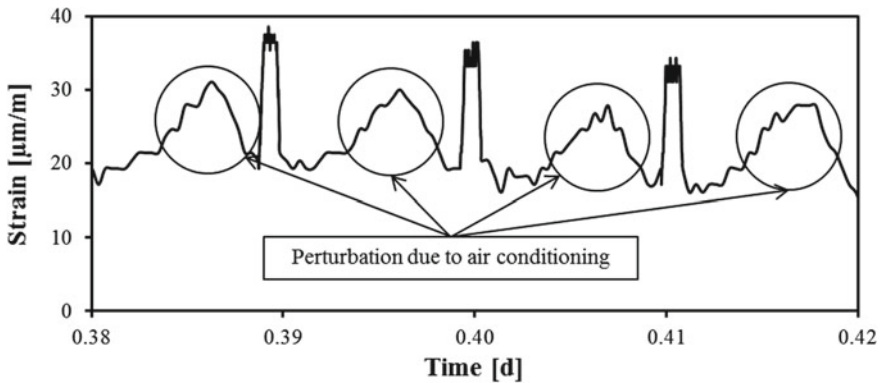
Fig. 6.17 Perturbation on the sensor of displacement caused by the air-conditioning
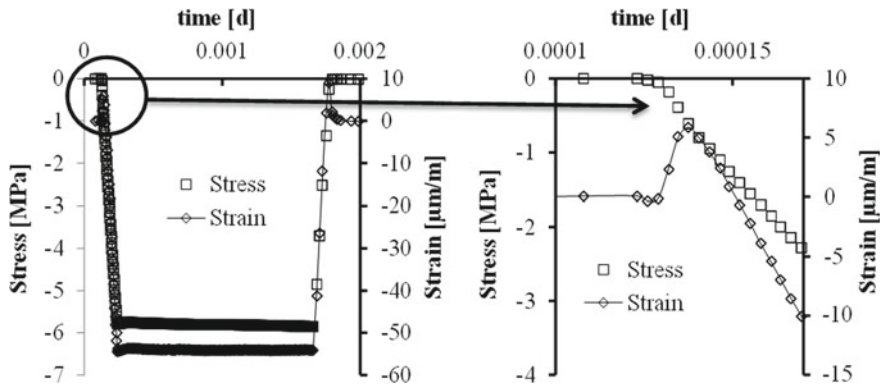
Fig. 6.18 Illustration of adherence/deterioration in the concrete around the stem anchorage in the sample

Young's modulus in tension and in compression. Damage by fatigue phenomenon is observed. A problem of adherence/deterioration was also observed for the anchorage of the stem as illustrated in Fig. 6.18 for one loading. During the beginning of loading, when a compressive load is applied to the sample, the stress increases as expected but the strain increases as if a tensile load is applied. Then the strain develops in the good direction. This problem is assumed to be a wobble in the sample due to damage around the anchorage. This phenomenon was observed in different concrete when repeated loadings are applied. The higher the W/C ratio and sooner this phenomenon appeared. For repeated loading, internal anchorage has to be disallowed.

For these reasons, a new experimental measurement tool was designed for the measurement of the longitudinal strain. This tool is an extensometer which is adapted to the TSTM device. The transversal measurement is added for the study of the Poisson's ratio and the creep dilatancy. Here are the different criteria which are on the basis of the design of the extensometer:

– For the limitation of the thermal dilation of the extensometer, all structural elements of the extensometer are in INVAR©.
– All elements for the measurement of longitudinal and transversal displacements have to be protected from the air conditioning.
– Sensors with a high accuracy are needed for the measurement of the transversal displacement. For this purpose, Solartron LE12 sensors (digital sensor) are used.
– External anchorages are used to avoid internal damage in the section of the concrete specimen. Three elastic anchorages from the J2P company (Boulay and Colson 1981) have been used to assure a good contact between the extensometer and the sample.
– Measurement of the transversal displacement has to be done in the same section as the anchorage to follow the longitudinal displacement and avoid artifacts of measurements.
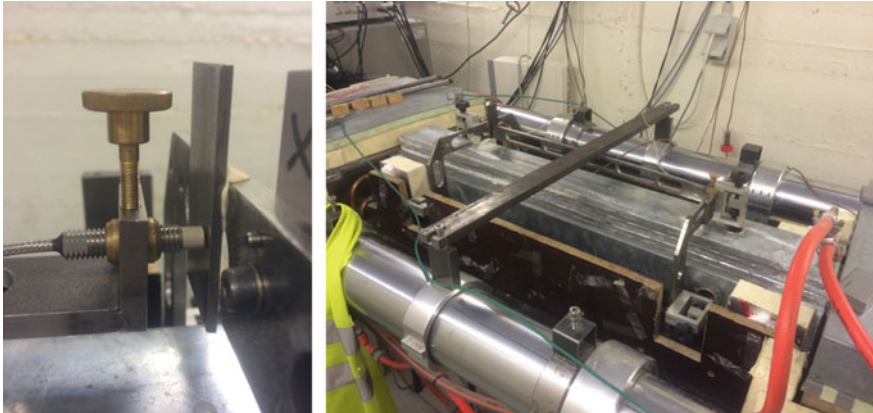
Fig. 6.19 New extensometer designed for the TSTM device

– A free lateral displacement of the specimen has to be allowed during the test to
avoid confinement effect when a compressive load is applied.

From these criteria, an extensometer composed of two parts with a U shape has
been designed. Figure 6.19 shows the new extensometer.

For the study of the restrained shrinkage since setting time, such instrumentation
cannot be used. Indeed, in that case the test must start just after the setting. The
implementation of the extensometer takes time and needs to remove the formwork.
For this reason, all tests can be performed with the new extensometer except test of
restrained shrinkage. For restrained shrinkage, anchorage rod system is used.

Finally, for the study of the restrained shrinkage under drying condition, the
upper part and/or the lateral part of the mold and the thermal regulation is removed
in order to expose the sample to the controlled environment (temperature and relative
humidity). To simulate the case of a slab, only the upper part of the thermal regulation
is removed (Bendimerad et al. 2020; Delsaute et al. n.d.) while the case of the
formwork removal of a wall is simulated by removing the lateral faces of the mold
and the thermal regulation.

6.4.2   Test Protocol for the Restrained Shrinkage

Historically, the TSTM was developed for the study of the restrained shrinkage. A
test method has been defined to measure the restrained shrinkage (Fig. 6.20). At
the beginning of the test, the sample placed in the TSTM is initially restraint by
the stiffness of the frame with the motor being turned off until the stress inside the
concrete reaches a threshold value of 0.01 MPa. At that moment, the displacement
transducer readings are set to zero and the concrete sample can deform freely until
the recorded deformation in the central part of the specimen reaches a deformation
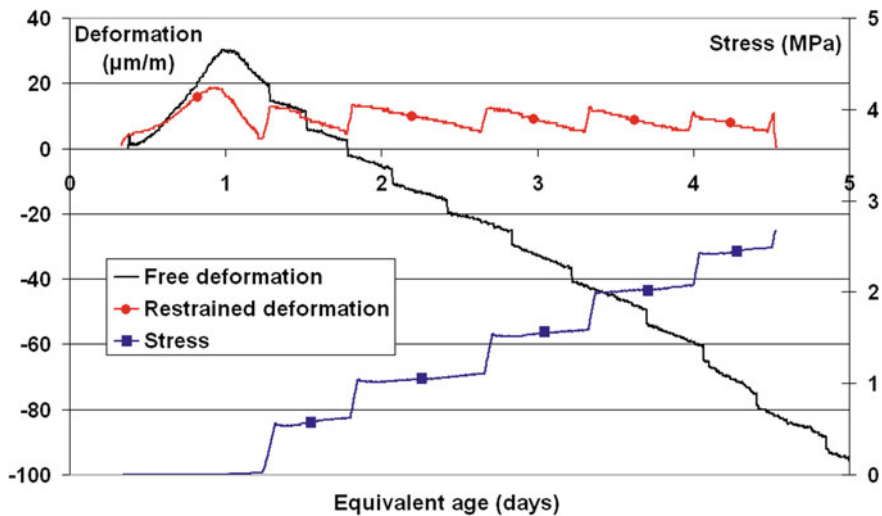
Fig. 6.20 Free and restrained shrinkage evolution of a Portland cement concrete and stress build-up in the concrete sample (Darquennes 2009)

threshold corresponding to 6.7 µm/m. This moment coincides with the end of the first cycle. From this time on, the load is adjusted to pull the specimen back to its initial length. Then, the applied load at the end of the adjustment process is kept constant throughout the following cycles until the sample deformation reaches again the deformation threshold value. The test goes on until the specimen cracks. This kind of experimental process is quite similar to the one used by Charron (2003) and allows avoiding an early cracking of the specimen. During this test, four parameters were continually monitored: the load applied on the sample, its deformation, its temperature and the displacement of the moving head. For concrete composition with high W/C ratio (Delsaute and Staquet 2017; Delsaute et al. 2016c) or high content of slag (Carette et al. 2018b) or in case of high increase of temperature due to hydration, a swelling is observed just after the final setting time. To consider the restrained of the swelling strain, the test protocol has been adapted (Carette et al. 2018a). The test starts at the final setting time. At that time the strains are set to zero. When the strain in the central part of the specimen reaches a strain threshold corresponding to −6.7 µm/m or +6.7 µm/m, a tensile or a compressive load is applied to put the specimen back to its initial length.

6.5 Applications

The use of TSTM devices was mainly related to the study of the restrained shrinkage at the laboratory scale on concrete as presented in the previous sections. However,

during this last decade, other kinds of TSTM devices were developed whether for industrial applications or for a better physical understanding of the physical mechanisms related to early age cracking of cementitious materials. Several new kinds of device and associated applications are presented succinctly below.

6.5.1 Monitoring of the Viscoelastic Properties Since Setting

As presented in Chap. 4, repeated minute-scale-duration loadings method was developed for the monitoring and the modelling of the viscoelastic properties of cement based materials in three laboratories: the Université Libre de Bruxelles (ULB), the Institut Français des Sciences et Technologies des Transports, de l'Aménagement et des Réseaux (IFSTTAR) and the Technische Universität Wien (TUWIEN). At ULB and Ifsttar, the main application of this test was to monitor and to model accurately the viscoelastic behavior at very early age (Boulay et al. 2012, 2013, 2014; Delsaute et al. 2012, 2013, 2014, 2016a, b, c, 2017; Delsaute and Staquet 2014; Staquet et al. 2014). In order to apply repeated loadings since the final setting time, a TSTM device was used at ULB. At TUWIEN, the new testing methodology was used for the identification of creep properties at the microstructural scale and also to study the water transfer between aggregate and cement paste during hydration (Ausweger et al. 2019; Göbel et al. 2018a, b; Irfan-ul-Hassan et al. 2016, 2017; Karte et al. 2015; Königsberger et al. 2016).

6.5.2 Implementation of Non-destructive Methods on a TSTM Device

To characterize experimentally the internal restriction of the cement paste caused by the aggregate, Pirskawetz et al. (2012) have developed a TSTM device which combines non-destructive methods. Ultrasound velocity method and acoustic emission have been integrated to the TSTM mold. These methods allow monitoring continuously the damage process in hardening material. Ultrasound velocity method characterizes the development of the microstructure during hardening while acoustic emission has been used to observe and detect the formation and the development of micro-cracks. The TSTM device was designed for cement paste and mortar (Fig. 6.21). The central part of the TSTM has a length of 34 cm and a cross section of 4 cm × 4 cm. Ultrasonic sensors are placed at the end of both extremities while the 3 acoustic emission sensors are put on the upper part of the measuring part.

It should be noticed that the first TSTM device designed for cement paste scale was developed in Delft University of Technology for the study of the development of the autogenous strain and the development of shrinkage-induced stresses (Lura 2003; Zhou et al. 2006). This device has a cross section of 7.5 mm × 7.5 mm and a measurement length of 37.5 mm.
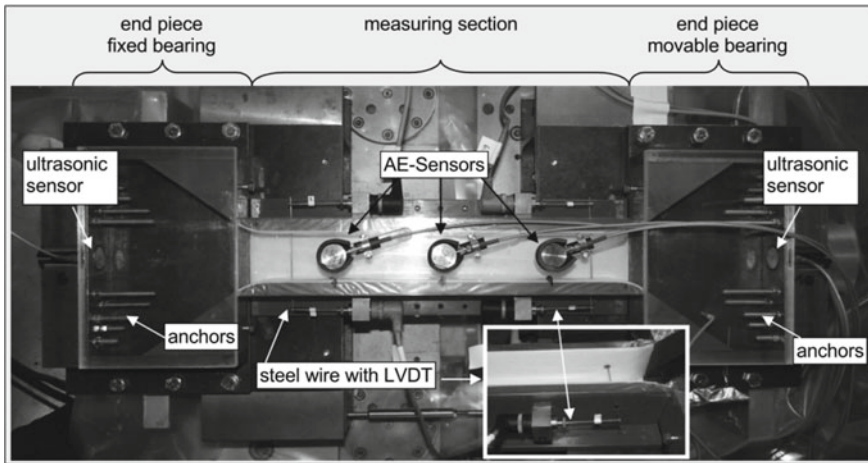
Fig. 6.21 TSTM device combining acoustic emission and ultrasound velocity method (Pirskawetz et al. 2012)

6.5.3 Testing Concrete in Its Plastic State

TSTM device were generally designed for the study of the behavior of cement based materials during the hardening phase. However, concrete elements, with a large exposed surface, are sensitive to cracking when concrete is still in a plastic state. Different curing procedures were developed to reduce the cracking risk of plastic concrete. One way to prevent cracking consists periodically in applying a fog spray on the exposed surface. Such method is responsible of wetting and drying cycles and thus causes variation of capillary pressure inside concrete. This corresponds to cyclic loadings of concrete during its plastic state. In order to simulate this situation, Khan (2018) and Khan et al. (2017) have developed a TSTM device which is enable to measure the tensile strength, and stress relaxation properties of plastic concrete as well as its resistance to cyclic loading till the end of setting. The device is shown in Fig. 6.22. The whole test setup is supported by a beam. The measurement length is 100 mm and the total length of the sample is 618 mm. One LVDT sensor is placed on the top of the specimen in the central part for the measurement of the concrete deformation. Concrete was tested in a climate control room.

6.5.4 Influence of Cyclic Loading/Displacement on the Hardening Process of Grout Material

The foundation of offshore wind turbines in a seabed is a major technical challenge for engineers. To insure the stability of the wind turbine, the ring between the steel
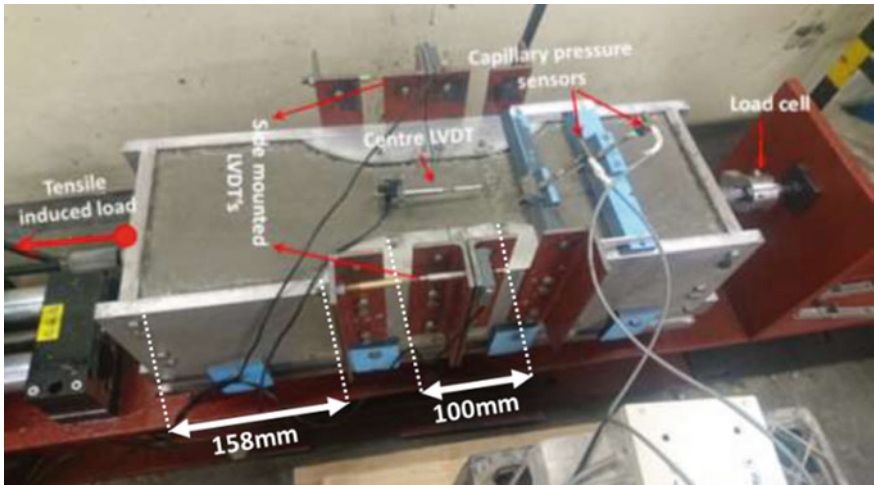
Fig. 6.22 TSTM device developed to study the influence of tensile cyclic loading and relaxation on plastic concrete (Khan 2018)

monopile and the seabed is filled with a grout. Since casting, the grouted connections have to carry the loadings resulting from waves acting on the monopile. As illustrated in Fig. 6.23, this leads to cycling loading of the grout and further to potential local damage in form of micro-cracks if the associated stress/strength ratio is high enough. The damage might accumulate over time and might eventually lead to a significant reduction of the local mechanical strength and local durability properties of the grout. In addition, the application of cyclic loadings can lead to irreversible plastic strain which can induce the formation of a gap at the interface between the monopile and the grouted connections (Lohaus et al. 2015). In order to point out the influence of early age movements and deformational restraints on the performance of a grouted connection, Delsaute (2019) and Delsaute et al. (2018) have developed a new testing methodology in which a TSTM device has been used. The test protocol was developed in order to reproduce the displacement/loading imposed by the waves on the grout
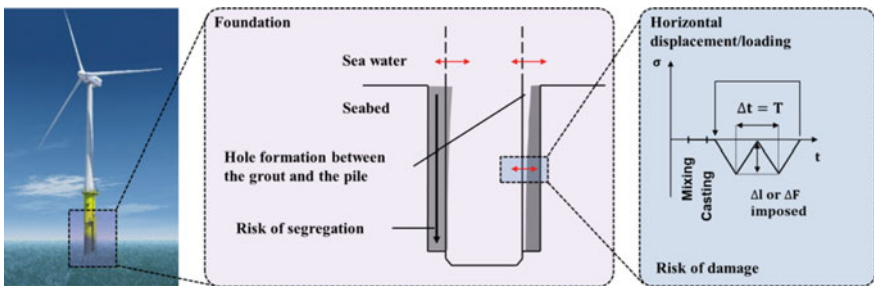
Fig. 6.23 Loading case induced by the cyclic movement of the wave on the grout (Delsaute 2019)

annulus during the construction process. Firstly, cyclic displacements are applied to the sample since an age of 1 h till the moment that a force threshold is reached (around the initial setting). Then cyclic loadings are applied on the sample. At this moment, displacement sensors were activated in order to monitor the displacement of the anchored rod in the straight part of the sample. From this moment, the recording of the displacement was used to compute the E-modulus for each loading and unloading. At an age of 24 h the cyclic loadings are stopped. At the end of the test, the prismatic part of the TSTM and dummy specimens were removed from the mold and were cut in several cubes of 10 cm side for the determination of the compressive strength. Compressive strength from both specimens are compared in order to define a potential strength reduction induced by the cyclic loading. Results of the E-modulus obtained by means of cyclic loading are then compare to the E-modulus obtained by means of repeated loadings in order to evaluate the potential damage of the grout. Finally, the free strains of the loaded specimen and the dummy specimen are also compared in order to quantify the irreversible strain induced by the application of cyclic loadings. From this new experimental protocol, new indicators were developed in order to evaluate the performance of grout materials under cyclic displacement and loading since casting.

6.5.5 Structural Scale

At the Technical University of Graz, a TSTM device has been elaborated at the structural scale. Such device was created for the development of a mechanically consistent design model for crack width concrete in restrained concrete members (Turner et al. 2015). For this purpose, the sample has a dog bone shape with a total length of 3.7 m and a cross section of 25 cm × 25 cm in the central part. The stiffness of the whole frame has been designed to simulate restrained shrinkage of reinforced concrete structure. In addition, hydraulic cylinders have been placed at one end of the steel columns and are used to impose displacement to the concrete member in order to simulate load variation induced by the seasonal temperature change. At the other end of the columns, a load cell was placed to monitor the force induced by the restrained of the free deformation of the concrete member and by the displacement imposed with the hydraulic cylinders. Finally, variable insulation system has been developed in order to simulate the thermal history of concrete element induced by hydration heat. Complete details about the test setup are given in the Chap. 7.

6.5.6 Degree of Restraint

Generally, in concrete structures, only a part of the free strains of concrete are restrained. 2D or 3D linear elastic calculation can be performed in order to evaluate the degree of restriction of a concrete element by the structure [see e.g. (Schlicke

and Matiašková 2019)]. Thus, the degree of restraint in early age concrete structure depends on the location of the concrete element and the general configuration of the structure (Klausen 2016). At NTNU, Klausen et al. (2015) have updated a TSTM device in order to control the degree of restraint R (between 0 and 100%) of a concrete sample. Also, the test protocol was adapted. When a measured length change in the TSTM exceeds a displacement threshold χ, a displacement is automatically applied to cancel partially the deformation and corresponds to $-R \cdot \chi$. The concrete sample can shrink again and the load is kept constant till a new length change of χ is reached. Then another partial compensation cycle $(-R \cdot \chi)$ begins. At Tsinghua University, Zhu et al. (2017, 2018) have developed a multiple TSTM system named "Synchronous closed loop federated control TSTM system". Four TSTM systems are placed in a same room which is controlled in temperature and relative humidity. The degree of restraint of each TSTM system can vary between 0 and 100% and the mold of each TSTM can be detached from the test rig. Such configuration allows casting the concrete directly on a construction site.

6.6 Conclusions

In this chapter, a succinct state-of-the-art of passive and active restrained shrinkage test method for the evaluation of the risk of cracking of cementitious materials under restrained condition has been presented. In the 1990s, a new experimental concrete testing concept has been designed: the Temperature Stress Testing Machine (TSTM). The device is able to monitor the mechanical behaviour of concrete since setting time under restrained conditions. Actually, the restrained shrinkage test set up designed with a TSTM system takes into account all the parameters affecting the stresses development inside the concrete sample: the degree of restriction, the relaxation of stresses, the evolution of the strength and the stiffness … On basis of this kind of test, several parameters can be quantified such as the elastic deformation, free and restrained shrinkages and also, creep and relaxation.

Between 1990 and 2010, less than fifteen laboratories worldwide have developed or acquired this kind of experimental equipment. All devices bear some similarities but major differences remain in the test set up designs (e.g. sample dimension, measurement length, instrumentation, thermal regulation), in the testing processes (test start, deformation threshold) and also in the scale of the material used (cement paste, mortar or concrete). Based on the development of several TSTM devices, a revisited TSTM system has been designed at ULB for monitoring the mechanical properties of concrete in tension and in compression since setting time. Several updates have been operated during this last decade in order to improve the device for the study of the restrained shrinkage and to extend its use to other applications. The design of this system includes a thermal regulation in contact with all sides of the concrete sample and, especially, for the very early age, displacement sensors without contact to limit the measurement artefacts on the concrete. A dummy mold was added to the revisited TSTM system for monitoring the free shrinkage and the thermal deformation.

So, the direct measurement of the creep deformation and the relaxation stresses is possible with the simultaneous use of the first and the dummy mold. The test method for measuring the early age properties of concrete must also avoid an early cracking of the concrete sample. To do so, the test method starts after the end of setting time of concrete when the stiffness of the studied material is sufficient.

This test device can offer much to the characterization of cement-based materials. Several types of tests can be performed according to the intended application. The TSTM device is able to simulate experimentally the situation of a concrete member (e.g. temperature, degree of restraint) which makes the TSTM a key tool for the study of the thermo-mechanical response of cement based materials since very early age.

References

Altoubat, S. A., & Lange, D. A. (2001). Creep, shrinkage, and cracking of restrained concrete at early age. *ACI Materials Journal, 98*(4), 323–331.

Altoubat, S. A., & Lange, D. A. (2002). Grip-Specimen interaction in uniaxial restrained tests. In *Concrete: Materials science to applications* (pp. 189–204), edited by ACI.

Aly, T., & Sanjayan, J. G. (2008). Shrinkage cracking properties of slag concretes with one-day curing. *Magazine of Concrete Research, 60*(1), 41–48.

Ausweger, M., Binder, E., Lahayne, O., Reihsner, R., Maier, G., Peyerl, M., et al. (2019). Early-age evolution of strength, stiffness, and non-aging creep of concretes: Experimental characterization and correlation analysis. *Materials, 12*(2), 207.

Baesens, P., & Delsaute, B. (2010). Comportement de Bétons Au Jeune Âge En Conditions de Déformations Libres et Restreintes. Université Libre de Bruxelles.

Banthia, N., Azzabi, M., & Pigeon, M. (1993). Restrained shrinkage cracking in fibre-reinforced cementitious composites. *Materials and Structures, 26*(7), 405–413.

Banthia, N., Azzabi, M., & Pigeon, M. (1995). Restrained shrinkage tests on fiber reinforced cementitious composites. *ACI Special Publication, 155,* 137–152.

Banthia, N., Yan, C., & Mindess, S. (1996). Restrained shrinkage cracking in fiber reinforced concrete: A novel test technique. *Cement and Concrete Research, 26*(1), 9–14.

Benboudjema, F., Carette, J., Delsaute, B., Honorio de Faria, T., Knoppik, A., Lacarrière, L., et al. (2019). Mechanical properties. In E. M. R. Fairbairn and M. Azenha (Eds.), *Thermal cracking of massive concrete structures—State of the art report of the rilem technical committee 254-CMS* (pp. 69–114).

Bendimerad, A. Z., Delsaute, B., Roziere, E., Staquet, S., & Loukili, A. (2020). Advanced techniques for the study of shrinkage-induced cracking of concrete with recycled aggregates at early age. *Construction and Building Materials*.

Bentur, A. (2003a). Evaluation of early age cracking characteristics in cementitious systems. *Materials and Structures, 36*(257), 183–190.

Bentur, A. (2003b). Terminology and definitions. In A. Bentur (Ed.), *Early age cracking in cementitious systems—Report of RILEM technical committee 181-EAS—Early age shrinkage induced stresses and cracking in cementitious systems* (pp. 13–15). RILEM Publications SARL.

Bjontegaard, O. (1999). Thermal dilation and autogenous deformation as driving forces to self-induced stresses in high-performance concrete.

Bloom, R., & Bentur, A. (1995). Free and restrained shrinkage of normal and high-strength concretes. *ACI Materials Journal, 92*(2), 211–217.

Boulay, C., & Colson, A. (1981). Un Extensomètre à Béton Éliminant l'influence Des Déformations Transversales Sur La Mesure Des Déformations Longitudinales. *Materials and Structures, 14*(79), 35–38.

Boulay, C., Crespini, M., Delsaute, B., & Staquet, S. (2012). Monitoring of the creep and the relaxation behaviour of concrete since setting time, Part 1 : Compression. In *Strategies for sustainable concrete structures* (p. 10). Aix-en-Provence.

Boulay, C., Staquet, S., Azenha, M., Deraemaeker, A., Crespini, M., Carette, J., et al. (2013). Monitoring elastic properties of concrete since very early age by means of cyclic loadings, ultrasonic measurements, natural resonant frequency of composite beam (EMM-ARM) and with smart aggregates. In *Proceedings of the 8th International Conference on Fracture Mechanics of Concrete and Concrete Structures, FraMCoS 2013*.

Boulay, C., Staquet, S., Delsaute, B., C, J., C, Michela, Yazoghli-Marzouk, O., et al. (2014). How to monitor the modulus of elasticity of concrete, automatically since the earliest age? *Materials and Structures, 47*(1–2), 141–155.

Bourchy, A. (2018). Relation Chaleur d'hydratation Du Ciment : Montée En Température et Contraintes Générées Au Jeune Âge Du Béton. Université Paris-Est.

Briffaut, M., Benboudjema, F., Torrenti, J. M., & Nahas, G. (2011a). A thermal active restrained shrinkage ring test to study the early age concrete behaviour of massive structures. *Cement and Concrete Research, 41*(1), 56–63.

Briffaut, M., Benboudjema, F., Torrenti, J. M., & Nahas, G. (2011b). Numerical analysis of the thermal active restrained shrinkage ring test to study the early age behavior of massive concrete structures. *Engineering Structures, 33*(4), 1390–1401.

Carette, J., Delsaute, B., & Staquet, S. (2018a). Estimating the stress development in early age concrete with mineral additions from coupled measurements. In *Interdisciplinary Approaches for Cement-based Materials and Structural Concrete: Synergizing Expertise and Bridging Scales of Space and Time* (pp. 171–176).

Carette, J., Joseph, S., Cizer, Ö., & Staquet, S. (2018b). Decoupling the autogenous swelling from the self-desiccation deformation in early age concrete with mineral additions: Micro-macro observations and unified modelling. *Cement and Concrete Composites, 85,* 122–132.

CEOS.fr. (n.d.). CEOS.Fr Comportement et Evaluation Des Ouvrages Spéciaux Vis-à-Vis de La Fissuration et Du Retrait." Retrieved January 23, 2019. https://www.ceosfr.irex.asso.fr/en/.

Charron, J. P. (2003). Contribution à l'étude Du Comportement Au Jeune Âge Des Matériaux Cimentaires En Conditions Des Déformations Libre et Restreinte. Ph.D. thesis, Université Laval.

Darquennes, A. (2009). Comportement Au Jeune Âge de Bétons Formulés à Base de Ciment Au Laitier de Haut Fourneau En Condition de Déformations Libre et Restreinte. Ph.D. thesis, Université Libre de Bruxelles.

Darquennes, A., Staquet, S., & Espion, B. (2006). Shrinkage of slag cement concrete in free and restrained conditions. In O. M. Jensen, P. Lura, & K. Kovler (Eds.), *International RILEM Conference on Volume Changes of Hardening Concrete: Testing and Mitigation* (p. 10).

Delsaute, B. (2016). New approach for monitoring and modelling of the creep and shrinkage behaviour of cement pastes, mortars and concretes since setting time. Université Libre de Bruxelles (BATir) and Université Paris Est (IFSTTAR).

Delsaute, B. (2019). Influence of cyclic movement on the hardening process of grout: case of offshore wind turbine installation. In G. Pijaudier-cabot, P. Grassl, & C. La Borderie (Eds.), *10th International Conference on Fracture Mechanics of Concrete and Concrete Structures, FraMCoS-X* (p. 11). Anglet.

Delsaute, B., Boulay, C., Granja, J., Carette, J., Azenha, M., Dumoulin, C., et al. (2016a). Testing concrete E-modulus at very early ages through several techniques: An inter-laboratory comparison. *Strain, 52*(2), 91–109.

Delsaute, B., Boulay, C., & Staquet, S. (2016b). Creep testing of concrete since setting time by means of permanent and repeated minute-long loadings. *Cement and Concrete Composites, 73,* 75–88.

Delsaute, B., Carette, J., & Staquet, S. (2013). Monitoring of the creep and the relaxation at very early age: Complementary results on the CEOS concrete. In *VIII International Conference on Fracture Mechanics of Concrete and Concrete Structures (IA-FramCOS-8)* (pp. 453–458).

Delsaute, B., Furnémont, R., Königsberger, M., & Staquet, S. (2018). Influence de Mouvement Cyclique Sur Le Durcissement de Coulis: Cas Des Éoliennes Offshores. In *19ème édition des Journées Scientifiques (RF) ^{2}B (Regroupement Francophone pour la Recherche et la Formation sur le Béton* (p. 10). Bayonne, France.

Delsaute, B., Hamami, A., Rozière, E., Staquet, S., & Loukili, A. (n.d.). Autogenous and drying shrinkage induced stresses in early age CEM I concrete – influence of the nature and the porosity of gravel. In *Cement and Concrete Composites*.

Delsaute, B., & Staquet, S. (2014). Early age creep and relaxation modelling of concrete under tension and compression. In *CONMOD 2014: Proceedings of the RILEM International Symposium on Concrete Modelling* (pp. 12–14).

Delsaute, B., & Staquet, S. (2017). Decoupling thermal and autogenous strain of concretes with different water/cement ratios during the hardening process. *Advances in Civil Engineering Materials, 6*(2).

Delsaute, B., & Staquet, S. (2019). Development of strain-induced stresses in early age concrete composed of recycled gravel or sand. *Journal of Advanced Concrete Technology, 17*(6), 319–334.

Delsaute, B., Staquet, S., & Boulay, C. (2012). Monitoring of the creep and the relaxation behaviour of concrete since setting time, Part 2 : Traction. In *Strategies for Sustainable Concrete Structures* (p. 10). Aix-en-Provence.

Delsaute, B., Staquet, S., & Boulay, C. (2014). Early age creep and relaxation behavior of concrete under tension and compression. In *Concrete Innovation Conference CIC 2014* (p. 10). Oslo.

Delsaute, B., Torrenti, J.-M., & Staquet, S. (2016c). Monitoring and modeling of the early age properties of the vercors concrete. In *TINCE 2016* (p. 12). Paris.

Delsaute, B., Torrenti, J. M., & Staquet, S. (2017). Modeling basic creep of concrete since setting time. *Cement and Concrete Composites, 83,* 239–250.

Dong, W., Yuan, W., Zhou, X., & Wang, F. (2018). The fracture mechanism of circular/elliptical concrete rings under restrained shrinkage and drying from top and bottom surfaces. *Engineering Fracture Mechanics, 189,* 148–163.

Göbel, L., Königsberger, M., Osburg, A., & Pichler, B. (2018a). Viscoelastic behavior of polymer-modified cement pastes: insight from downscaling short-term macroscopic creep tests by means of multiscale modeling. *Applied Sciences, 8*(4), 487.

Göbel, L., Osburg, A., & Pichler, B. (2018b). The mechanical performance of polymer-modified cement pastes at early ages: Ultra-short non-aging compression tests and multiscale homogenization. *Construction and Building Materials, 173,* 495–507.

Grazia, T. (1999). Comportement Des Bétons Au Jeune Âge. Ph.D. thesis, Université Laval.

He, Z., Zhou, X., & Li, Z. (2004). New experimental method for studying early-age cracking of cement-based materials. *ACI Materials Journal, 101*(1), 50–56.

Hossain, A. B., & Weiss, J. (2004). Assessing residual stress development and stress relaxation in restrained concrete ring specimens. *Cement and Concrete Composites, 26*(5), 531–540.

Hossain, A. B., & Weiss, J. (2006). The role of specimen geometry and boundary conditions on stress development and cracking in the restrained ring test. *Cement and Concrete Research, 36*(1), 189–199.

Igarashi, S. I., Bentur, A., & Kovler, K. (2000). Autogenous shrinkage and induced restraining stresses in high-strength concretes. *Cement and Concrete Research, 30*(11), 1701–1707.

Irfan-ul-Hassan, M., Königsberger, M., Reihsner, R., Hellmich, C., & Pichler, B. (2017). How water-aggregate interactions affect concrete creep: Multiscale analysis. *Journal of Nanomechanics and Micromechanics, 7*(4).

Irfan-ul-Hassan, M., Pichler, B., Reihsner, R., & Hellmich, Ch. (2016). Elastic and creep properties of young cement paste, as determined from hourly repeated minute-long Quasi-Static tests. *Cement and Concrete Research, 82,* 36–49.

Jaafri, R., Samouh, H., Roziere, E., Alam, S. Y., Wisniewski, V., & Loukili, A. (2019). Experimental and numerical analysis of curling behavior of natural hydraulic lime—Cement based mortars. *Cement and Concrete Research, 117,* 1–15.

Ji, G. M., Kanstad, T., & Bjøntegaard, Ø. (2018). Calibration of material models against TSTM test for crack risk assessment of early-age concrete containing fly ash. *Advances in Materials Science and Engineering, 9,* 1–11.

Kamen, A., Denarié, E., Sadouki, H., & Brühwiler, E. (2008). Thermo-mechanical response of UHPFRC at early age—Experimental study and numerical simulation. *Cement and Concrete Research, 38*(6), 822–831.

Kanavaris, F., Azenha, M., Soutsos, M., & Kovler, K. (2019). Assessment of behaviour and cracking susceptibility of cementitious systems under restrained conditions through ring tests: A critical review. *Cement and Concrete Composites, 95,* 137–153.

Karte, P., Hlobil, M., Reihsner, R., Dörner, W., Lahayne, O., Eberhardsteiner, J., et al. (2015). Unloading-based stiffness characterisation of cement pastes during the second, third and fourth day after production. *Strain, 51*(2), 156–169.

Khan, M.Y. (2018). *The tensile material properties of plastic concrete and the influence on plastic cracking*. Stellenbosch University.

Khan, M. Y., Kolawole, J. T., Boshoff, W. P., & Combrinck, R. (2017). Influence of relaxation and cyclic loading on the tensile material properties of plastic concrete. In S. Staquet & D. G. Aggelis (Eds.) *2nd International RILEM/COST Conference on Early Age Cracking and Serviceability in Cement-based Materials and Structures (EAC2)* (pp. 379–384). RILEM Publications S.A.R.L.

Kishi, T., & Lin, Z. (2008). A tentative experimental evaluation on early-age creep. In *Creep, shrinkage and durability mechanics of concrete and concrete structures* (pp. 285–291).

Klausen, A. B. E. (2016). *Early age crack assessment of concrete structures: Experimental investigation of decisive parameters*. NTNU.

Klausen, A. E., Kanstad, T., & Bjøntegaard, Ø. (2015). Updated temperature-stress testing machine (TSTM): Introductory tests, calculations, verification, and investigation of variable fly ash content. In *CONCREEP 2015: Mechanics and Physics of Creep, Shrinkage, and Durability of Concrete and Concrete Structures—Proceedings of the 10th International Conference on Mechanics and Physics of Creep, Shrinkage, and Durability of Concrete and Concrete Structure*.

Königsberger, M., Irfan-ul-Hassan, M., Pichler, B., & Hellmich, C. (2016). Downscaling based identification of nonaging power-law creep of cement hydrates. *Journal of Engineering Mechanics, 142*(12), 04016106.

Kovler, K. (1994). Testing system for determining the mechanical behaviour of early age concrete under restrained and free uniaxial shrinkage. *Materials and Structures, 27*(6), 324–330.

Kovler, K., & Bentur, A. (2009). *Cracking sensitivity of normal- and high-strength concrete*.

Kovler, K., Sikuler, J., & Bentur, A. (1993). Restrained shrinkage tests of fibre-reinforced concrete ring specimens: Effect of core thermal expansion. *Materials and Structures, 26*(4), 231–237.

Lohaus, L., Cotardo, D., Werner, M., Schaumann, P., & Kelma, S. (2015). Experimental and numerical investigations of grouted joints in monopiles subjected to early-age cycling. *Journal of Ocean and Wind Energy, 2*(4).

Lokhorst, S. J. (1998). *Deformational behaviour of concrete influenced by hydration related changes of the microstructure*.

Lura, P. (2003). *Autogenous deformation and internal curing of concrete*. Ph.D. thesis, Delft University of Technology.

Melo Neto, A. A., Cincotto, M. A., & Repette, W. L. (2007). *Desenvolvimento de Metodologia e Equipamento Para a Medida Da Retração Restringida*. Brazil.

Paillere, A. M., Buil, M., & Serrano, J. J. (1989). Effect of fiber addition on the autogenous shrinkage of silica fume concrete. *ACI Materials Journal, 86*(2), 139–144.

Pirskawetz, S., Weise, F., & Fontana, P. (2012). Analysis of early-age cracking of cementitious materials by combination of various non destructive testing methods. In *2nd International Conference on Microstructural-related Durability of Cementitious Composites* (pp. 350–359).

Rilem 42-CEA. (1981). Properties of set concrete at early ages state-of-the-art-report. *Matériaux et Constructions, 14*(6), 399–450.

RILEM TC 119-TCE. (1997). Avoidance of thermal cracking in concrete at early ages—Recommendations. *Materials and Structures, 30*, 451–461.

Schlicke, D., Matiašková, L. (2019). Advanced computational methods versus analytical and empirical solutions for determining restraint stresses in bottom-restrained walls. *Journal of Advanced Concrete Technology, 17*, 335–349.

Schlitter, J. L., Barrett, T., & Weiss, W. J. (2010a). Restrained shrinkage behavior due to combined autogenous and thermal effects in mortars containing super absorbent polymer (Sap). In *International RILEM Conference on Use of Superabsorbent Polymers and Other New Additives in Concrete* (August).

Schlitter, J. L., Senter, A. H., Bentz, D. P., Nantung, T., & Weiss, W. J. (2010b). A dual concentric ring test for evaluating residual stress development due to restrained volume change. *Journal of ASTM International, 7*(9), 103118.

Schöppel, K., Plannerer, M., & Springenschmid, R. (1994). Determination of restraint stresses and of material properties during the hydration of concrete with temperature-stress testing machine. In *RILEM Proceedings 25, Thermal Cracking in Concrete at Early Ages*.

Springenschmid, R., Breitenbücher, R., & Mangold, M. (1994). Development of the cracking frame and the temperature-stress testing machine. In *RILEM Proceedings 25, Thermal Cracking in Concrete at Early Ages* (pp. 137–144).

Staquet, S., Azenha, M., Boulay, C., Delsaute, B., Carette, J., Granja, J., et al. (2014). Maturity testing through continuous measurement of E-modulus: An inter-laboratory and inter-technique study. In *Proceedings of ECO-CRETE International Symposium on Sustainability* (p. 8).

Staquet, S., Delsaute, B., Fairbairn, E. M. R., Torrent, R., Knoppik, A., Ukrainczyk, N., et al. (2019). *Mixture Proportioning for Crack Avoidance* (vol. 27).

Turcry, P. (2004). Retrait et Fissuration Des Bétons Autoplaçans : Influence de La Formulation. Université de Nante.

Turner, K., Schlicke, D., & Tue, N. V. (2015). Restraint and crack width development during service life regarding hardening caused stresses. In *Proceeding of the fib Symposium* (pp. 1–8). Copenhagen, Denmark.

Vaysburd, A. M., Emmons, P. H., Bissonnette, B., & Pigeon, M. (2001). Some aspects of evaluating cracking sensitivity of repair materials. In K. Kovler & A. Bentur (Eds.), *RILEM Proceedings PRO 23 Early Age Cracking in Cementitious Systems—EAC'01* (pp. 169–185). RILEM Publications S.A.R.L.

Weiss, J., Lura, P., Rajabipour, F., & Sant, G. (2008). Performance of shrinkage-reducing admixtures at different humidities and at early ages. *ACI Materials Journal, 105*(5), 478–486.

Weiss, W. J., & Shah, S. P. (2002). Restrained shrinkage cracking: the role of shrinkage reducing admixtures and specimen geometry. *Materials and Structures, 35*(246), 85–91.

Weiss, J., Yang, W., & Shah, S. (2000). Influence of specimen size/geometry on shrinkage cracking of rings. *Journal of Engineering Mechanics, 126*(3), 233–242.

Yokoyama, K., Hiraishi, S., Kasai, Y., & Kishitani, K. (1994). Shrinkage and cracking of high-strength concrete and flowing concrete at early ages. In *ACI Special Publication* (vol. 148, pp. 243–258).

Zhou, X., Dong, W., & Oladiran, O. (2014). Experimental and numerical assessment of restrained shrinkage cracking of concrete using elliptical ring specimens. *Journal of Materials in Civil Engineering, 26*(11), 04014087.

Zhou, J., Ye, G., Schlangen, E., & Van Breugel, K. (2006). Autogenous deformation of portland cement paste blended with blast furnace slag measured by mini-TSTM. In *International RILEM Conference on Volume Changes of Hardening Concrete: Testing and Mitigation* (pp. 367–374, vol. C).

Zhu, H., Li, Q., Hu, Y., & Ma, R. (2018). Double feedback control method for determining early-age restrained creep of concrete using a temperature stress testing machine. *Materials, 11*(7), 1079.

Zhu, H., Li, Q., & Yu, H. (2017). Self-developed testing system for determining the temperature behavior of concrete. *Materials, 10*(4), 419.